



**HAL**  
open science

# ARP Interleavers for Decomposed Parallel Concatenated Convolutional Codes

Mohammad Bazzal, Jérémy Nadal, Stefan Weithoffer, Charbel Abdel Nour,  
Catherine Douillard

► **To cite this version:**

Mohammad Bazzal, Jérémy Nadal, Stefan Weithoffer, Charbel Abdel Nour, Catherine Douillard. ARP Interleavers for Decomposed Parallel Concatenated Convolutional Codes. IMT Atlantique. 2025. ⟨hal-05166912⟩

**HAL Id: hal-05166912**

**<https://imt-atlantique.hal.science/hal-05166912v1>**

Submitted on 17 Jul 2025

HAL is a multi-disciplinary open access archive for the deposit and dissemination of scientific research documents, whether they are published or not. The documents may come from teaching and research institutions in France or abroad, or from public or private research centers.

L'archive ouverte pluridisciplinaire HAL, est destinée au dépôt et à la diffusion de documents scientifiques de niveau recherche, publiés ou non, émanant des établissements d'enseignement et de recherche français ou étrangers, des laboratoires publics ou privés.



Distributed under a Creative Commons CC BY 4.0 - Attribution - International License

# ARP Interleavers for Decomposed Parallel Concatenated Convolutional Codes

Mohammad Bazzal, Jeremy Nadal, Stefan Weithoffer, Charbel Abdel Nour, Catherine Douillard  
 IMT Atlantique, Lab-STICC, UMR CNRS 6285, F-29238 Brest, France

**Abstract**—This technical document provides a short description of a novel structure for parallel concatenated convolutional codes (PCCCs), originally proposed in [1] as *decomposed PCCC* (DPCCC). To ease result reproducibility, the full list of interleaver parameters used for evaluating the DPCCC structure in [1] are provided in this document. These interleavers were designed to maximize the minimum Hamming distance (mHD) and lower the error floor compared to conventional PCCC structures, such as turbo codes, by partitioning the input frame into subframes, each independently interleaved and encoded. This decomposition targets mHD codewords, partly through mitigating the quadratic increase in the multiplicity of periodic input weight-2 sequences, thus lowering their probability of co-occurrence in the component codes. Simulation results demonstrate that the proposed DPCCC structure, combined with the tailored interleaver design, achieves competitive performance compared to other code classes, with notable improvements in mHD and error floor performance over TCs, while maintaining rate compatibility and supporting low-latency decoder architectures.

At high SNRs, the error correction performance of conventional parallel concatenated convolutional codes (PCCCs) is constrained by their minimum Hamming Distance (mHD), with low distance leading to high error floors [2]. For TCs, low-weight codewords are generated when a low-weight input sequence forms a Return-to-Zero (RTZ) sequence in each component convolutional encoders. Such sequences are referred to as Turbo RTZ (TRTZ) sequences in [3].

To mitigate the occurrence of low-weight TRTZ sequences, thereby improving the mHD of the code, a novel PCCC structure is proposed in [1], referred to as decomposed PCCC (DPCCC). Such a structure is presented in Figure 1. The first parity output of length  $K$  is generated by encoding the original information frame  $\mathbf{d}_1$  using encoder  $C_1$ . The frame  $\mathbf{d}_1$  is then uniformly partitioned into  $\mathcal{L} = n_{cc} - 1$  subframes, denoted by  $(\mathbf{d}'_2, \dots, \mathbf{d}'_{n_{cc}})$ . Each subframe  $\mathbf{d}'_q$  ( $q \in [2, n_{cc}]$ ) is formed by selecting bits from  $\mathbf{d}_1$  according to the following indexing rule:

$$\mathbf{d}'_q[\ell] = \mathbf{d}_1[\ell\mathcal{L} + q - 2], \quad \forall \ell < K/\mathcal{L} - 1 \quad (1)$$

The size of each decomposed subframe  $\mathbf{d}'_q$  is given by  $\lfloor K/\mathcal{L} \rfloor$ . Each subframe  $\mathbf{d}'_q$  is interleaved using  $\Pi_q$  to produce  $\mathbf{d}_q$ , which is subsequently encoded by constituent encoder  $C_q$ . The interleaver of the first subframe ( $q = 1$ ) is set to the identity function ( $\Pi_1(i) = i$ ), and for the  $q \geq 2$  remaining subframes, ARP interleavers are considered in this document [4]:

$$\Pi_q(i) = \text{mod}_K(P_q \times i + S_q(\text{mod}_Q(i))), \quad (2)$$

with  $P_q$  a positive integer relatively prime to  $K$ ,  $Q$  is the disorder degree and  $S_q = (S_q(0), \dots, S_q(Q-1))$  is a tuple of

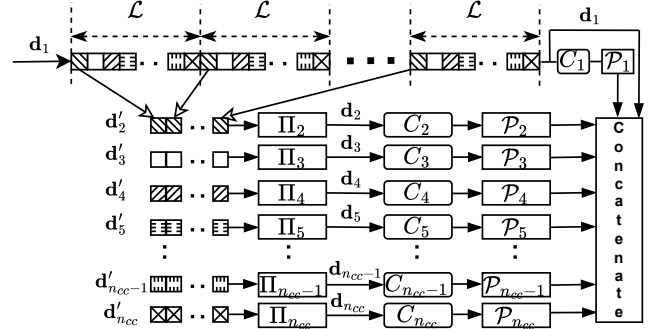


Fig. 1: Overview of the proposed DPCCC structure.

$Q$  elements containing the shift values of the ARP interleaver.

The overall code rate  $\mathcal{R}$ , without puncturing, is  $1/3$ , comprising  $K$  bits from the systematic stream,  $K$  from the first parity, and  $K$  from all subframe parities—matching the rate of conventional TCs. To support higher code rates, appropriate puncturing masks  $\mathcal{P}_q$  can be applied. For lower code rates ( $\mathcal{R} \leq 1/3$ ), the subframe size can be increased to  $\alpha K/\mathcal{L}$ , where  $\alpha = 1/\mathcal{R} - 2$ , by extracting additional bits from  $\mathbf{d}_1$ . This approach ensures rate flexibility while preserving the structural advantages of the decomposition. Therefore, the DPCCC scheme is fully defined by the number of decompositions  $\mathcal{L}$  and tuple  $\delta = (\Pi_q, C_q, \mathcal{P}_q)_{q \in [1, n_{cc}]}$ .

To evaluate the proposed DPCCC structure, several interleavers were designed (Table I) for various decomposition factors  $\mathcal{L}$  and frame sizes at a code rate of  $\mathcal{R} = 1/3$ . In addition, two configurations of RSC component codes are considered:

- a single-parity code using polynomial  $G_1 = G(1, \frac{15}{13})_8$ . No bits are punctured.
- a double-parity code using polynomial  $G_2 = G(1, \frac{15}{13}, \frac{17}{13})_8$  with systematic<sup>1</sup> (data) and parity puncturing to preverse the global code rate at  $\mathcal{R} = 1/3$ . The data puncturing pattern is [10100000], the parity puncturing patterns are respectively [11101111] for the first parity outputs (polynomial  $\frac{15}{13}$ ) and [01011010] for the second parity outputs (polynomial  $\frac{17}{13}$ ).

Table II reports the estimated mHD for different DPCCC decompositions, compared against LTE baselines. Figure 2 presents the FER performance for various DPCCC config-

<sup>1</sup>Systematic data puncturing has been shown to increase the mHD of TCs, enhancing performance in the error floor region [4], at the cost of degraded performance in the waterfall region.

**TABLE I:** Parameters of ARP interleavers designed for various decomposition factors, and frame sizes, using a fixed interleaver period  $Q = 4$  for coding rate  $\mathcal{R} = 1/3$ .

$\mathcal{R}$	$K$	$G$	$\mathcal{L}$	$[P_q]_{q \in [2, n_{cc}]}$	$[S_q(0), \dots, S_q(Q-1)]_{q \in [2, n_{cc}]}$	
1/3	128	$G_1$	2	[29,29]	[(2,14,34,46),(1,15,21,59)]	
			4	[19,11, 27,11]	[(3,29,28,4),(2,16,18,0), (3,6,22,17),(0,12,20,20)]	
			8	[3,9, 3,9, 1,1, 13,3]	[(0,6,9,1), (0,2,3,7), (2,4,10,0), (3,1,15,13), (0,8,8,12), (2,12,5,5), (0,13,9,14), (1,3,10,14)]	
			16	[3,7, 3,3, 1,3, 5,7, 5,3, 3,1, 7,5, 3,1]	[(3,1,7,5), (3,7,6,0), (1,0,2,5), (0,2,1,5), (1,6,4,5), (1,4,0,7), (1,6,0,1), (1,3,5,3), (0,5,3,0), (3,2,2,1), (1,4,2,5), (0,1,7,4), (0,4,3,1), (0,4,5,7), (2,2,6,2), (3,1,7,5)]	
			$G_2$	2	[51, 5]	[(0,7,63,54),(1,11,61,35)]
			1024	$G_1$	2	[119,363]
		4			[163,231, 89,95]	[(3,19,147,227),(3,141,231,41), (2,211,209,186),(3,86,210,189)]
		8			[77,53, 125,121, 63,23, 7,85]	[(1,114,46,11), (3,103,119,39), (1,86,18,43), (1,13,54,92), (3,118,80,87), (0,0,60,0), (0,72,108,52), (1,86,46,11)]
		16		[5,11, 3,55, 25,21, 1,31, 17,59, 53,47, 61,11, 39,13]	[(1,14,46,55), (1,5,8,22), (3,62,16,11), (0,34,53,33), (1,58,52,53), (2,51,31,44), (3,51,3,23), (0,14,53,61), (1,53,21,53), (0,30,8,22), (2,54,27,29), (1,1,32,6), (2,48,37,37), (3,27,54,0), (3,37,56,20), (0,16,36,4)]	
		$G_2$		4	[239,117, 159,187]	[(3,242,122,9),(1,233,141,89), (2,188,174,196),(1,204,176,107)]
		6144		$G_1$	2	[2143, 1199]
			4		[53,1165, 521,149]	[(1,334,1226,423),(1,523,981,871), (0,52,1244,1448),(0,132,653,1255)]
	8		[443,535, 11,445, 527,341, 197,271]		[(2,356,106,344), (0,707,709,324), (1,505,585,409), (2,528,353,661), (2,185,313,752), (3,619,644,386), (0,89,315,736), (1,256,166,113)]	
	16		[169,241, 101,343, 113,287, 191,133, 329,305, 115,167, 167,347, 365,215]		[(1,102,314,195), (1,102,292,329), (1,69,78,292), (0,276,195,21), (2,31,39,268), (0,79,343,2), (3,377,268,72), (1,2,128,289), (2,167,47,172), (2,148,74,16), (1,97,264,362), (1,132,178,333), (2,206,134,230), (3,242,274,253), (0,72,153,287), (2,336,74,300)]	
	$G_2$		8		[713,415, 661,287, 55,65, 715,709]	[(0,412,521,267), (2,218,121,67), (1,150,580,301), (1,216,676,135), (3,425,660,240), (1,542,760,529), (0,220,743,613), (0,486,611,547)]

urations using  $G_1$  and the best configurations using  $G_2$ . Simulations were conducted in an AWGN channel with BPSK modulation and a maximum of 8 max-log-MAP (MLM) decoding iterations at  $\mathcal{R} = 1/3$ .

For benchmarking, we include LTE TCs, 5G low-density parity-check (LDPC) codes—decoded with 20 iterations of the layered offset min-sum algorithm [5]—and polar codes designed using AFF3CT [6] and decoded via successive cancellation list-32 (SCL-32). Simulation results at high SNRs align with the mHD estimates in Table II. For  $K = 128$  with  $G_1$ , the  $\mathcal{L} = 2$  configuration achieves the best FER, outperforming all baselines. For  $K = 1024$ , the configurations  $\mathcal{L} = 2$  and  $\mathcal{L} = 4$  deliver the best performance. At  $K = 6144$ ,

**TABLE II:** Estimated mHD (method in [3]) of LTE TC and the proposed DPCCC across various decomposition factors  $\mathcal{L}$  and frame length  $K$ .

	$K = 128$		$K = 1024$		$K = 6144$	
	$G_1$	$G_2$	$G_1$	$G_2$	$G_1$	$G_2$
$\mathcal{L} = 2$	<b>28</b>	<b>32</b>	<b>46</b>	48	50	48
$\mathcal{L} = 4$	26	31	<b>46</b>	<b>56</b>	<b>51</b>	60
$\mathcal{L} = 8$	24	30	45	54	<b>57</b>	<b>72</b>
$\mathcal{L} = 16$	18	19	42	47	54	64
LTE	16		27		26	

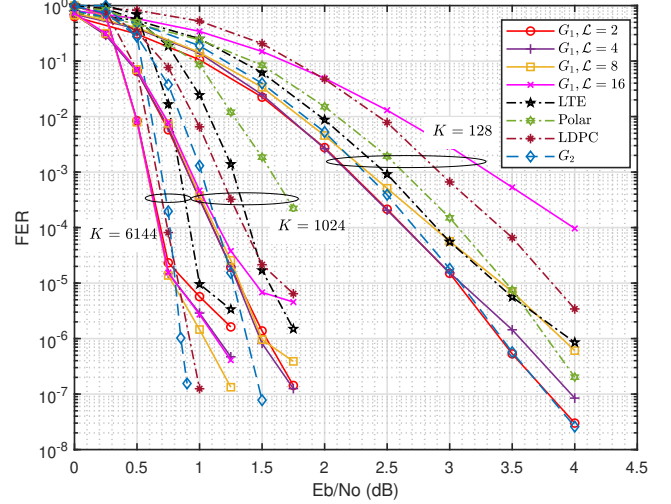


**Fig. 2:** FER performance of the proposed DPCCC using RSC with generator polynomial  $G_1$  and the best decomposition factors  $\mathcal{L}$  (from Table II) with  $G_2$ , for various frame sizes.

the 5G LDPC outperforms DPCCC  $G_1$  at higher SNRs, while the proposed DPCCC with  $G_2$  surpasses both. Although  $G_2$  exhibits slightly degraded performance at low SNR due to systematic puncturing, it consistently outperforms  $G_1$ , LTE, polar, and LDPC codes at higher SNRs. This confirms the effectiveness of the DPCCC structure and interleaver design.

## REFERENCES

- [1] M. Bazzal, J. Nadal, S. Weithoffer, C. Abdel Nour, and C. Douillard, "A Novel Parallel Concatenated Convolutional Code Structure Based on Frame Decomposition," in *IEEE Int. Symp. on Topics in Coding 2025*, Los Angeles, August, [Accepted for publication].
- [2] L. Perez, J. Seghers, and D. Costello, "A distance spectrum interpretation of turbo codes," *IEEE Trans. Inf. Theory*, vol. 42, no. 6, pp. 1698–1709, Nov. 1996.
- [3] M. Bazzal, J. Nadal, S. Weithoffer, C. Abdel Nour, and C. Douillard, "Efficient decoder-free minimum distance estimation for concatenated convolutional codes," in *IEEE Veh. Technol. Conf.*, Oslo, July 2025.
- [4] R. Garzón-Bohórquez, C. Abdel Nour, and C. Douillard, "Protograph-Based Interleavers for Punctured Turbo Codes," *IEEE Trans. Commun.*, vol. 66, no. 5, pp. 1833–1844, Dec. 2018.
- [5] D. Hui, S. Sandberg, Y. Blankenship, M. Andersson, and L. Grosjean, "Channel Coding in 5G New Radio: A Tutorial Overview and Performance Comparison with 4G LTE," *IEEE Veh. Technol. Mag.*, vol. 13, no. 4, pp. 60–69, Oct. 2018.
- [6] A. Cassagne, O. Hartmann, M. Léonardon, K. He, C. Leroux, R. Tajan, O. Aumage, D. Barthou, T. Tonnellier, V. Pignoly, B. Le Gal, and C. Jégo, "AFF3CT: A Fast Forward Error Correction Toolbox!" *Elsevier SoftwareX*, vol. 10, p. 100345, Oct. 2019.